Lecithin hydrophobicity modulates the process of cholesterol crystal nucleation and growth in supersaturated model bile systems

Hidenori OCHI, Susumu TAZUMA* and Goro KAJIYAMA

First Department of Internal Medicine, Hiroshima University School of Medicine, Hiroshima, Japan

The present study was performed to determine whether the degree of lecithin hydrophobicity regulates bile metastability and, therefore, affects the process of cholesterol crystallization. Supersaturated model bile (MB) solutions were prepared with an identical composition on a molar basis (taurocholate/lecithin/cholesterol, 73:19.5:7.5; total lipid concentration 9 g/dl) except for the lecithin species; egg yolk phosphatidylcholine, soybean phosphatidylcholine, 1-palmitoyl-2-linoleoyl-*sn*-phosphatidylcholine, dilinoleoyl phosphatidylcholine and dipalmitoyl phosphatidylcholine. Each MB solution was incubated and sequentially examined. Video-enhanced contrast microscopy demonstrated that the rate of vesicular aggregation and fusion correlated with the degree of lecithin hydrophobicity, and that the rate of cholesterol crystal nucleation correlated with the degree of lecithin hydrophilicity. In MBs containing less hydrophobic lecithin, needle-like crystals developed and transformed into mature plate-like crystals, whereas classical plate-like crystals were consistently observed in MBs composed of hydrophobic lecithin. Laser-diffraction particle size analysis demonstrated that the increase in lecithin hydrophobicity enlarged the vesicle dimension, enhancing its cholesterol-holding capacity. Correlation between vesicular cholesterol packing density and lecithin hydrophobicity suggests that the process of bile cholesterol nucleation and growth is regulated, in part, by acyl chain unsaturation in lecithin. Since the composition of biliary lecithins is responsive to dietary manipulations, this study provides new insights into the prevention of cholesterol gallstones.

INTRODUCTION

Recent studies have indicated that changes in the molecular species of lecithin in bile may be important in the solubility of cholesterol (CH) in bile and the pathogenesis of CH gallstone formation in man [1,2]. We have reported that the degree of unsaturation of lecithin in model bile (MB) systems affects bile metastability, which is reflected by CH crystal nucleation [3]. CH is solubilized in vesicles as well as mixed micelles in bile, particularly when the concentration of CH exceeds its micellar solubility [4]. These vesicles may play an important role in the process of CH crystal nucleation. Several studies have demonstrated that CH crystal nucleation originates from aggregation and fusion of CH-rich vesicles [5]. We have reported that CH crystal nucleation was not always preceded by vesicular aggregation in supersaturated MB systems [3]. On the other hand, Konikoff et al. have demonstrated that CH did not nucleate plate-like monohydrate crystals directly from dilute MB systems [6]. In the present study, we have analysed the effect of the hydrophobicity of biliary lecithin on bile metastability and the CH crystal nucleation process using video-enhanced contrast microscopy and laser-diffraction particle size analysis.

MATERIALS AND METHODS

Preparation of MB solutions

CH was obtained from Wako Jyunyaku Co. (Osaka, Japan) and stored under nitrogen at 4 °C. Egg yolk phosphatidylcholine (EYPC), soybean phosphatidylcholine (SBPC) and 1-palmitoyl-2-linoleoyl-*sn*-phosphatidylcholine (PLPC), dilinoleoyl phosphatidylcholine (DLPC) and dipalmitoyl phosphatidylcholine (DPPC) were from the Sigma Chemical Co. (St. Louis, MO, U.S.A.) and stored at −80 °C. Sodium taurocholate (TCA) (Sigma) was recrystallized twice according to the method of Pope [7] prior to use. MB solutions were prepared according to a previously described method [8]. Aliquots of stock solutions (TCA in methanol, lecithin in chloroform/methanol, and CH in chloroform/methanol) were mixed in a volumetric flask and shaken at 37 °C overnight. Then the mixture was evaporated under a stream of nitrogen, lyophilized, and stored at −80 °C. Finally, the dried lipid film was resuspended in the appropriate volume of Hepes/NaCl (10 mM/150 mM) buffer containing 4 mM EDTA and 0.02% NaN_3 (pH 7.5). The mixture was flushed with nitrogen and shaken at 55 °C until microscopically isotropic. Five types of MB solutions containing natural lecithin or synthetic lecithin were prepared with an identical molar ratio of lipid components (taurocholate/lecithin/CH, 73:19.5:7.5; total lipid concentration 9 g/dl). This ratio of lipid components is physiologically found in the human gallbladder bile, and provides a physical chemical metastability of biliary lipid particulate species.

CH crystal growth assay

Quantitative assay of the appearance and growth of CH crystals was performed with a slight modification of the original method of Busch et al. [9]. The isotropic MB solutions were filtered through a sterile 0.45-μm-pore-size filter (Toyo Roshi, Tokyo), flushed with nitrogen and incubated in sealed 1 ml glass microvials at 37 °C. Time zero of nucleation was defined as 15 min after thermal equilibration. A 40 μl aliquot of each MB solution was sampled and diluted with Hepes/NaCl buffer containing 30 mM TCA. After 20 min, the absorbance was measured at

Abbreviations used: CH, cholesterol; DLPC, dilinoleoylphosphatidylcholine; DPPC, dipalmitoylphosphatidylcholine; EYPC, egg yolk phosphatidylcholine; MB, model bile; PLPC, 1-palmitoyl-2-linoleoyl-*sn*-phosphatidylcholine; SBPC, soybean phosphatidylcholine; TCA, sodium taurocholate.

* To whom correspondence should be addressed.

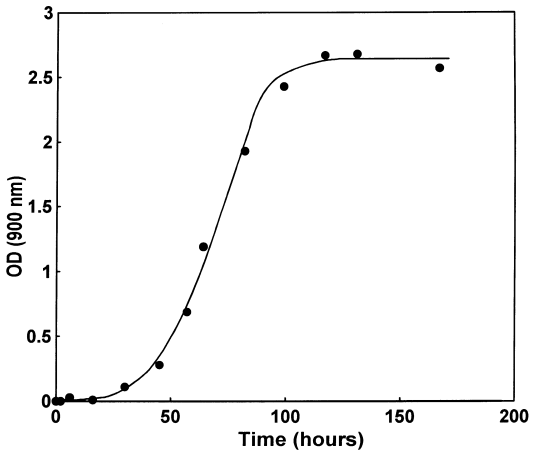

Figure 1 CH crystal growth curve

Based on this curve, the growth rate was calculated as follows: a linear line was adjusted to the sigmoidal curve tangentially. The slope of this linear line was used as a growth rate.

Table 1 CH crystal growth rate of MB solutions in this study

Values are means ± S.D. ($n = 3$).

MB solution	Growth rate (absorbance units/h)
DLPC-MB	0.161 ± 0.022
SBPC-MB	0.063 ± 0.013
PLPC-MB	0.046 ± 0.007
EYPC-MB	0.005 ± 0.001
DPPC-MB	–

900 nm using a spectrophotometer (UV-160, Shimadzu, Kyoto, Japan). Measurements were performed at different time intervals over a period of 600 h, depending on the crystal growth rate of the sample.

Video-enhanced contrast microscopic studies

One drop (≈ 10 μl) of MB solution was placed between two cover glasses at frequent intervals during incubation. The samples were observed at 37 °C using video-enhanced contrast microscopy (LABOPHOTO-2, Nikon, Tokyo, Japan). Images were monitored using a video camera control system (C-2400, Hamamatsu Photonics, Hamamatsu, Japan) with a video monitor (PMV-1442Q, Sony, Tokyo, Japan) and recorded on a videotape unit (BR-S811, Victor, Yokohama, Japan).

Dimensional analysis

The dimensions of lipid particles in MB solutions were measured using a laser-diffraction particle size analyser (SALD-2000, Shimadzu, Kyoto, Japan) [10]. Measurements were performed at different time intervals until the equilibrium state of the sample was reached.

HPLC analysis of lecithins

Lecithin hydrophobicity was determined by the retention times on reverse-phase HPLC (Shimadzu LC-6A system, Shimadzu

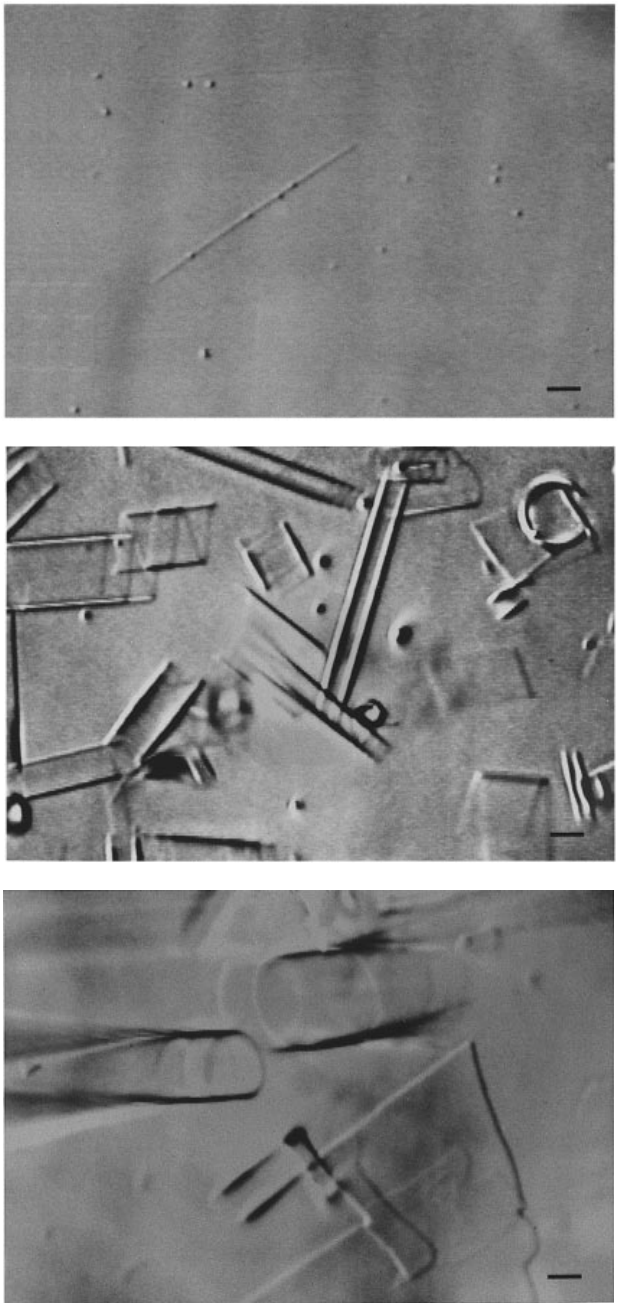

Figure 2 Particles present in DLPC-MB observed by video-enhanced contrast microscopy

Upper panel (**A**): Occasional vesicles and needle-like crystals observed at 2 h. Middle panel (**B**): Spiral or tube-like structures observed at 8 h. Lower panel (**C**): Plate-like crystals observed at 36 h. Scale bars = 10 μm.

Instruments, Tokyo, Japan) as previously described [11]. Lecithins were chromatographed on a 4.5 mm × 250 mm Ultrasphere 5 μm ODS column (Shimadzu) equipped with a 4.5 mm × 50 mm precolumn of the same material (Shimadzu Techno-Research, Tokyo, Japan) and eluted with methanol/water/acetonitrile solvent (90.5:7:2.5, by vol.) containing 20 mM choline chloride. Solvents were HPLC-grade and filtered (0.45 μm; Corning, Tokyo, Japan) prior to use. The flow rate was 2.0 ml/min and absorbance was monitored at 205 nm. The hydrophobic index of

each lecithin was calculated from the relative retention factors determined by retention times.

RESULTS

CH crystal growth assay

Figure 1 shows a representative CH crystal growth curve. The growth rate of each MB is shown in Table 1. The growth rate was found to have the rank order DLPC-MB > SBPC-MB > PLPC-MB > EYPC-MB. DPPC showed no crystal growth by 500 h.

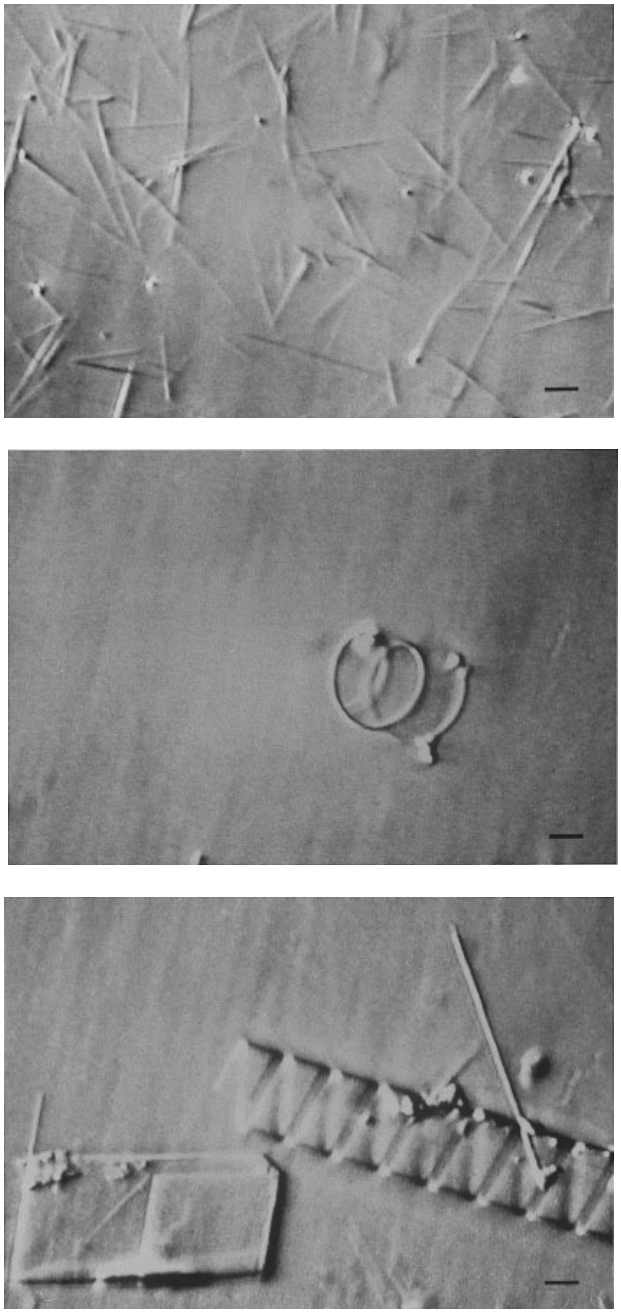

Figure 3 Particles present in SBPC-MB observed by video-enhanced contrast microscopy

Upper panel (**A**): Needle-like crystals observed at 5 h. Middle panel (**B**): Spiral crystals observed at 10 h. Lower panel (**C**): Plate-like crystals observed at 60 h. Scale bars = 10 μm.

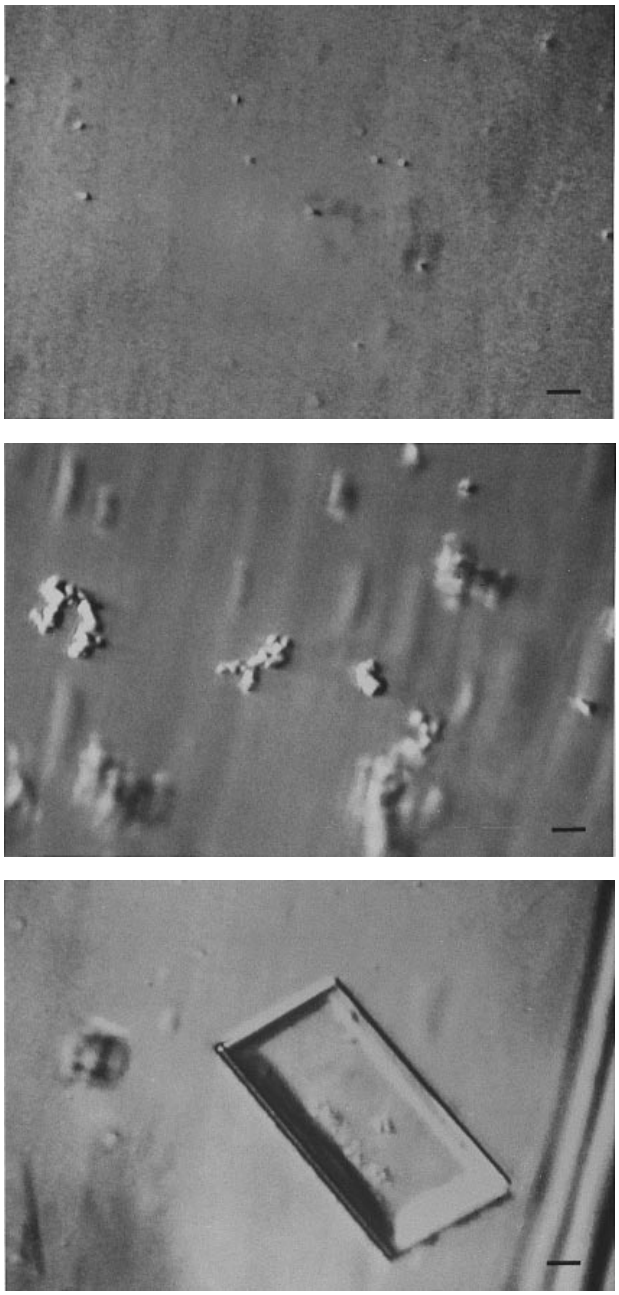

Figure 4 Particles present in EYPC-MB observed by video-enhanced contrast microscopy

Upper panel (**A**): Vesicles visible at 30 min. Middle panel (**B**): Large aggregates of vesicles observed at 2 h. Lower panel (**C**): Plate-like crystals initially observed at 60 h. Scale bars = 10 μm.

Estimation of the metastability of MB solutions

In DLPC-MB, we found a small amount of formation of vesicles and needle-like crystals almost simultaneously at 2 h (Figure 2A). Subsequently, these vesicles were dissolved at a strikingly rapid rate and needle-like crystals transformed into spiral shapes at 8 h (Figure 2B). At 36 h, plate-like crystals were the pre-

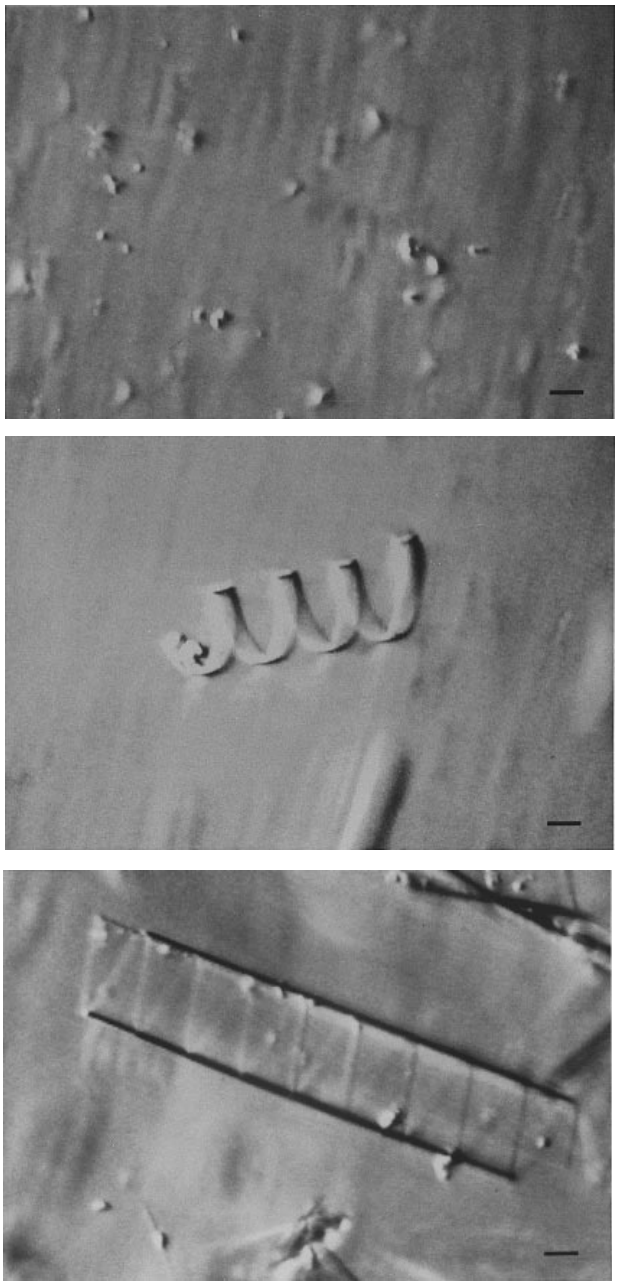

Figure 5 Particles present in PLPC-MB observed by video-enhanced contrast microscopy

Upper panel (**A**): Vesicular aggregates observed at 5 h. Middle panel (**B**): Spiral crystals observed at 20 h. Lower panel (**C**): Tube-like crystals observed at 50 h. Scale bars = 10 μm.

dominant form (Figure 2C). SBPC-MB showed similar but slower morphological alterations. A few vesicles were observed after 2–4 h. The rates of their aggregation and fusion were very slow. Following initiation of crystal nucleation, vesicles gradually disappeared. At 5 h, needle-like crystals were observed (Figure 3A). This was followed by growth along the long axis. Individual needles extended in length to several hundred micrometers with a width of less than 0.5 μm. During the next 10 h, spiral crystals appeared. Some grew laterally to become tube-like structures (Figure 3B). Finally, at 60 h, classical plate-like crystal growth

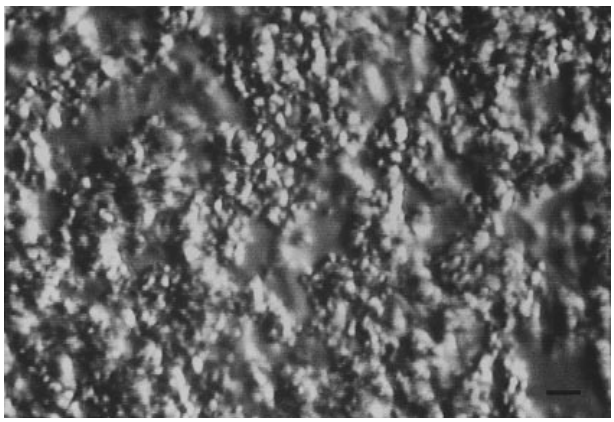

Figure 6 Particles present in DPPC-MB observed by video-enhanced contrast microscopy

Marked aggregation of vesicles was observed at 30 min.

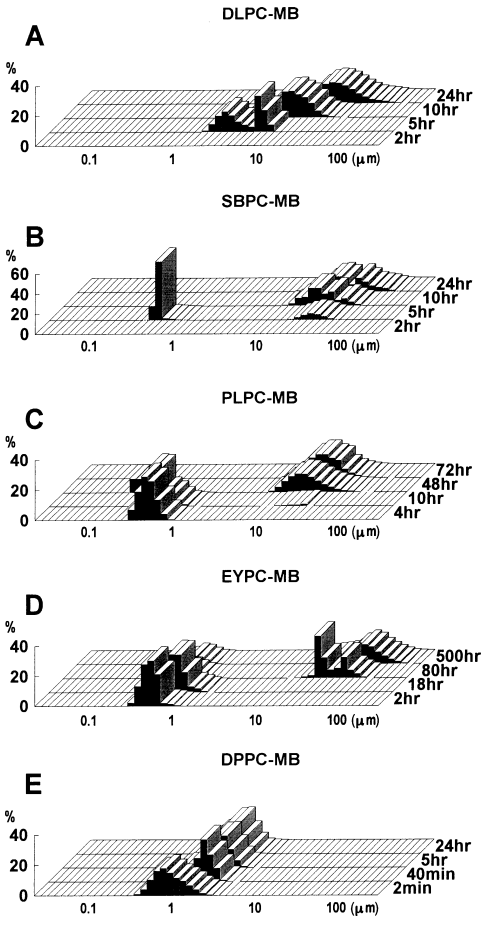

Figure 7 Size distribution of vesicles and crystals in MB solutions calculated by a laser-diffraction particle size analyser

The *y* axes show relative amounts of particles by total particle numbers. Vesicles and/or CH crystals in each MB were detected.

Table 2 Percentage molecular composition and hydrophobic index of lecithin by HPLC

The retention time (RT) of 16:0-18:2 PC (PLPC) was used as a reference. Relative hydrophobicity of each lecithin species was defined from the relative retention times (RRT) of HPLC and the hydrophobic index (HI) of each lecithin was calculated.

Lecithin species	RT (min)	RRT	DLPC (%)	SBPC (%)	PLPC (%)	EYPC (%)	DPPC (%)
18:2-18:3	12.6	0.55	–	10	–	–	–
18:2-18:2	17.1	0.75	100	42	–	–	–
16:0-20:4	22.3	0.97	–	–	–	6	–
16:0-18:2	22.9	1	–	23	100	19	–
18:1-18:2	25.3	1.11	–	9	–	–	–
16:0-18:1	30.8	1.35	–	2	–	38	–
18:0-20:4	36.2	1.58	–	–	–	7	–
18:0-18:2	37.8	1.65	–	6	–	8	–
16:0-16:0	40.8	1.78	–	–	–	–	100
18:0-18:1	52.1	2.27	–	–	–	9	–
Hydrophobic index...			0.8	0.9	1	1.4	1.8

was the predominant feature (Figure 3C). In EYPC-MB, by contrast, vesicle formation and aggregation were more rapid and abundant than in SBPC-MB (Figures 4A and 4B). Even at equilibrium, some vesicle aggregates still remained. As shown in Figure 4(C), initiation and growth of CH monohydrate crystals were very slow. Moreover, video-enhanced microscopy revealed that plate-like crystals formed from the early stages of nucleation in EYPC-MB. In PLPC-MB, the process of both aggregation of vesicles and nucleation of CH crystals displayed features that were intermediate to those of SBPC-MB and EYPC-MB (Figures 5A–5C). DPPC-MB showed massive aggregation of vesicles soon after incubation, followed by the absence of crystal formation (Figure 6).

Dimensions of vesicles and CH crystals in MBs

The time course of particle size distribution for each MB solution is shown in Figure 7. Particles with a diameter of 0.6–1.0 μm were vesicles and their aggregates. Particles with larger dimensions of 10–100 μm represented CH crystals. In DLPC-MB, rapid crystal growth without vesicular formation was observed. In SBPC-MB, vesicles of relatively small dimension were detected only at the initiation of crystal nucleation. In EYPC-MB, on the other hand, vesicular formation was detected soon after incubation. Vesicles gradually grew until the early stages of crystal precipitation and then slightly decreased in diameter. In DPPC-MB, no crystal precipitation was found following rapid aggregation of vesicles. The rank order of the maximum dimensions of vesicles was DPPC-MB > EYPC-MB > PLPC-MB > SBPC-MB.

The degree of hydrophobicity of various lecithin species by HPLC

The molar percentages of phosphatidylcholine molecular species in each lecithin used in the study are reported in Table 2. The retention time of 16:0–18:2 PC (PLPC) was used as a reference, and the retention time of the other species was divided by that of 16:0–18:2. Based on the weighted average of relative retention times of phosphatidylcholines, the overall hydrophobic index (HI) of each lecithin was estimated. The rank order of HI of lecithin species used in this study was DPPC (1.8) > EYPC (1.4) > PLPC (1.0) > SBPC (0.90) > DLPC (0.80).

DISCUSSION

Recent findings suggest that biliary phospholipids play a crucial role in solubilization of CH in bile. Jungst et al. have shown that increased phospholipid concentrations in bile had a greater effect on the CH nucleation than increased bile acid concentrations [12,13]. Halpern et al. have demonstrated that disaturated synthetic lecithins prolonged the nucleation time in comparison with egg lecithin or monounsaturated lecithins [14]. Molecular species of lecithin are asymmetrically distributed between vesicles and micelles in human bile and MB systems [15,16]. The results of this study demonstrated that lecithin hydrophobicity within a physiological range considerably affects bile metastability as well as the CH crystal nucleation process.

Several investigators have reported that CH crystals nucleate from vesicles in bile [5,17]. However, Ahrendt et al. have reported that CH is carried exclusively in, and nucleates rapidly from, mixed micelles without forming vesicles in the CH-fed prairie dog [18]. In the present study, CH crystals originate predominantly from mixed micelles in SBPC-MB and exclusively in DLPC-MB. These results support the theory that CH–phospholipid vesicles are not required for nucleation. Furthermore, time-lapse study using a video-enhanced contrast microscopy and laser-diffraction particle size analysis revealed that in MB systems containing less hydrophobic lecithins, such as SBPC-MB, vesicles formed occasionally and were followed by rapid CH crystal precipitation. In contrast, with more hydrophobic lecithin such as EYPC-MB, crystal nucleation occurred slowly compared with that of SBPC-MB despite massive vesicle aggregation. The degree of vesicle aggregation was inversely correlated with the rate of crystal nucleation. The mean diameter of vesicles reached a maximum at the onset of nucleation in most MB systems. CH crystal precipitation was suppressed while the vesicles grew, and once nucleation occurred, vesicle size was reduced (Figure 7). From these observations, vesicle formation appears to retard crystal precipitation, particularly when they consist of hydrophobic lecithins, incorporating excess CH molecules from other lipid particles and gradually releasing them. Furthermore, as vesicles fuse and grow in diameter, the more planar lipid bilayer may retain CH molecules. This theory is not consistent with the current concept that CH crystal nucleation originates from the fusion and aggregation of vesicles. It has been reported that several factors accelerate vesicle fusion and CH nucleation. Such fusion may not cause CH nucleation but

may counteract increased bile metastability, although further studies are needed to clarify the role of vesicles in greater detail.

Time-lapse microscopic study also revealed that CH crystals do not always nucleate plate-like crystals in supersaturated MB systems within physiological lipid compositions, and that lecithin hydrophobicity modulates this process. In dilute bile-salt-rich systems, Konikoff et al. have demonstrated that biliary CH does not nucleate classic monohydrate plates, and that lecithin molecular species may affect crystal habit [6,19]. Thus, its physiological relevancy was determined in the present study. Also, such crystal habits in native bile may be affected by bile acid composition [20]. Although the mechanisms of growth of immature needle-like or spiral crystals into typical plate-like crystals, as well as their significance in the pathogenesis of gallstone formation, are not yet defined, our findings support their possible application to native bile.

Since all experiments in the present study were performed using MB solutions with a single bile acid concentration, its relevancy to events which occur in the native bile might be limited. Nevertheless, we deduce that the fact that lecithin hydrophobicity affects bile metastability as well as the process of CH crystal nucleation and growth in supersaturated MB systems advances our understanding of the pathogenesis of gallstone formation.

Parts of this study have been presented as part of the 93rd Annual Meeting of the American Gastroenterological Association, San Francisco, May 10, 1992, the 94th Annual Meeting of the American Gastroenterological Association, Boston, May 15–21, 1993, and the 95th Annual Meeting of the American Gastroenterological Association, New Orleans, May 15, 1994.

Received 1 March 1996/15 April 1996; accepted 26 April 1996

REFERENCES

1 Kajiyama, G., Kubota, S., Sasaki, H., Kawamoto, T. and Miyoshi, A. (1980) Hiroshima J. Med. Sci. **20**, 133–141
2 Ahlberg, J., Curstedt, T., Einarsson, K. and Sjovall, J. (1981) J. Lipid Res. **22**, 404–409
3 Tao, S., Tazuma, S. and Kajiyama, G. (1993) Biochim. Biophys. Acta. **1167**, 142–146
4 Somjen, G. J. and Gilat, T. (1983) FEBS Lett. **156**, 265–268
5 Collins, J. and Phillips, M. C. (1982) J. Lipid Res. **23**, 291–298
6 Konikoff, F. M., Chung, D. S., Donovan, J. M., Small, D. M. and Carey, M. C. (1992) J. Clin. Invest. **90**, 1155–1160
7 Pope, J. L. (1967) J. Lipid Res. **8**, 146–147
8 Tazuma, S. and Holzbach, R. T. (1987) Proc. Natl. Acad. Sci. U.S.A. **84**, 2052–2056
9 Busch, N., Tokumo, H. and Holzbach, R. T. (1990) J. Lipid Res. **31**, 1903–1909
10 Tazuma, S., Ochi, H., Teramen, K., Yamashita, Y., Horikawa, K., Miura, H., Hirano, N., Sasaki, M., Aihara, N., Hatsushika, S., Tao, S., Ohya, T. and Kajiyama, G. (1994) Biochim. Biophys. Acta **1215**, 74–78
11 Patton, G. M., Fasulo, J. M. and Robins, S. J. (1982) J. Lipid Res. **23**, 190–196
12 Jungst, D., Lang, T. and Paumgartner, G. (1989) Hepatology **10**, 599
13 Jungst, D., Lang, T., Huber, T., Lange, V. and Paumgartner, G. (1993) J. Lipid Res. **34**, 1457–1464
14 Halpern, Z., Moshkowitz, M., Laufer, H., Peled, Y. and Gilat, T. (1993) Gut **34**, 110–115
15 Cohen, D. E. and Carey, M. C. (1991) J. Lipid Res. **32**, 1291–1302
16 Booker, M. L., LaMorte, W. W., Ahrendt, S. A., Lillemore, K. D. and Pitt, H. A. (1992) J. Lipid Res. **33**, 1485–1492
17 Halpern, Z., Dudley, M. A., Kibe, A., Lynn, M. P., Breuer, A. C. and Holzbach, R. T. (1986) Gastroenterology **90**, 875–885
18 Ahrendt, S. A., Fox-Talbot, K., Kaufman, H. S., Lillemoe, K. D. and Pitt, H. A. (1994) Biochim. Biophys. Acta **1211**, 7–13
19 Konikoff, F. M., Cohen, D. E. and Carey, M. C. (1994) J. Lipid Res. **35**, 60–70
20 Stolk, M. F. J., van de Heijining, B. J. M., van Erpecum, K. J., van den Broek, A. M. W. C., Renooij, W. and van Berge-Henegouwen, G. P. (1994) J. Hepatol. **20**, 802–810